



Wear Behaviors of a Ti-Based Bulk Metallic Glass at Elevated Temperatures

Fuyang Cao, Yongjiang Huang*, Chao He, Hongbo Fan, LiYuan Wei, Zhiliang Ning and Jianfei Sun

School of Materials Science and Engineering, Harbin Institute of Technology, Harbin, China

Bulk metallic glasses (BMGs) often offer excellent physical, chemical, and mechanical properties such as high strength, high hardness, and good wear/corrosion resistance, stemming from their unique atomic configuration. These properties enable them to be a potential engineering material in a range of industrial applications. However, the wear behaviors must be considered in structural applications. Here, the wear tests of a TiZrNiCuBe bulk metallic glass at high temperatures were carried out. As the testing temperature increases, the wear rate of the studied BMG sample gradually decreases and the sample surface becomes smoother. Meanwhile, a higher applied normal load causes a higher wear rate. The wear mechanism evolves from the abrasive to adhesive mode with increase in the testing temperature. The results obtained here could shed more insights into the deformation mechanism of BMGs and thus extend their industrial uses in high-temperature environments.

Keywords: metallic glasses, wear, high temperature, microstructure, deformation mechanism

OPEN ACCESS

Edited by:

Liqiang Wang,
Shanghai Jiao Tong University, China

Reviewed by:

Weiming Yang,
China University of Mining and
Technology, China
Jiang Ma,
Shenzhen University, China

*Correspondence:

Yongjiang Huang
yhuang@hit.edu.cn

Specialty section:

This article was submitted to
Structural Materials,
a section of the journal
Frontiers in Materials

Received: 15 April 2021

Accepted: 31 May 2021

Published: 22 June 2021

Citation:

Cao F, Huang Y, He C, Fan H, Wei L,
Ning Z and Sun J (2021) Wear
Behaviors of a Ti-Based Bulk Metallic
Glass at Elevated Temperatures.
Front. Mater. 8:695840.
doi: 10.3389/fmats.2021.695840

INTRODUCTION

During the last decades, bulk metallic glasses (BMGs), also termed as bulk amorphous metals, have attracted considerable scientific and industrial interests from materials science community due to their excellent physical, chemical, and mechanical properties (Greer, 1995; Schuh et al., 2007; Huang et al., 2009; Huang et al., 2010a; Zheng et al., 2011; Han et al., 2018; Liu et al., 2018; Lu et al., 2018; Li et al., 2019). Owing to their disordered atomic configuration differing from conventional crystalline materials, BMGs often offer ultrahigh strength, excellent wear/corrosion resistance, and high elastic limit, typically superior to those of their crystalline counterparts (Huang et al., 2010b; Edwards et al., 2013; Huang et al., 2014a; Louzguine-Luzgin et al., 2017; Yang et al., 2020). These fantastic properties make BMGs promising for structural applications (Axinte, 2012; Li et al., 2013; Wang et al., 2014; Shakur Shahabi et al., 2015; Hubek et al., 2020). Nowadays, wear failure in industrial applications is one of the key issues resulting in the damage of the engineering materials (Sun et al., 2006). As a kind of advanced materials, considerable attention has been paid to the tribological properties of BMGs, stemming from their excellent mechanical performance (Greer et al., 2002; Louzguine-Luzgin et al., 2016). A lot of studies involving the wear and friction behaviors of various BMGs, such as Zr- (Huang et al., 2014b; Zhao et al., 2018), Cu- (Maddala et al., 2010), Mg- (Hua et al., 2017), and Ti- (Duan et al., 2011) based alloys, have been reported until now. BMGs are demonstrated to possess excellent tribological properties, manifested by a low wear rate and low coefficient of friction (COF), suggesting their great potentials for industrial applications in friction components under severe friction and wear conditions (Khun et al., 2016). For instance, the durability of an Ni-based BMG

microgear was found to be typically 313 times longer than that of the conventional SK-steel gears (Ishiba et al., 2007), and the bearing rollers of Zr-based BMG showed a better wear resistance than the commercial GCr15 ones (Ma et al., 2004). (Prakash, 2005) stated that the wear characteristics of Co-, Fe-, and Ni-based BMGs were marginally superior to those of 304 stainless steel. Many research groups also studied the effect of experimental parameters such as surface roughness (Rahaman et al., 2015), surface modification (Matthews et al., 2007), sliding velocity (Huang et al., 2010b), and normal load (Zhong et al., 2015) on the friction and wear behaviors of BMGs. (Zhong et al., 2015) mentioned that the COF and wear rate of a $Zr_{41}Ti_{14}Ni_{10}Cu_{12.5}Be_{22.5}$ glass increased with both the sliding velocity and the normal load. For industrial applications, it is of essence to understand how a BMG behaves under elevated temperature conditions. Although previous literatures suggested that the friction and wear behaviors of BMGs are closely related with the testing temperatures (Rahaman et al., 2014; Huang et al., 2011), the high-temperature wear mechanism remains unclear so far. In this study, wear behaviors of a Ti-based BMG are studied at elevated temperatures. The effect of testing temperatures on the wear performance is studied. It is expected that the results obtained here could shed more insights into the wear mechanism of BMGs and thus extend their applications in high-temperature load-bearing environments.

EXPERIMENTAL PROCEDURES

The master ingots with a $Ti_{40}Zr_{25}Ni_3Cu_{12}Be_{20}$ (at. %) nominal composition were prepared by arc-melting the mixtures of pure Ti, Zr, Ni, Cu, and Be metals with purities higher than 99.9 wt. % under a Ti-gettered argon atmosphere. In order to achieve homogeneity of the chemical composition, the alloy ingots were remelted at least four times. Bulk alloy rods of 6 mm in diameter and ~60 mm in length were then fabricated by suction-casting the alloy melt into a copper mold. The samples of 8 mm in length for high-temperature wear tests were electrical-discharge machined from the as-cast alloy cylindrical samples. Both the top and bottom surfaces of all the alloy samples were then carefully ground and polished to a mirror finish in order to obtain identical surface roughness. Then the BMG samples were ultrasonically cleaned in ethanol for 10 min and dried under warm air flow. Abrasive ball-on-plate wear tests were conducted on an HT-1000 universal wear machine at high temperatures. Prior to the wear tests, the BMG alloy samples and ceramic balls were heated and kept at a set temperature for 10 min to achieve a steady temperature field within the heating chamber. The ambient temperature was maintained within ± 1 K during high-temperature wear tests. The applied normal loads were selected to be 1.5, 2.5, or 3.5 N, respectively. The sliding velocity employed was selected to be 600 r/min. The counter body was Si_3N_4 ceramic ball with 6.3 mm in diameter. New ceramic balls were used for each test. The COF was continuously recorded during the wear tests by a computer. At least five wear tests were carried out at each condition, and the results presented in this article had the standard deviation of less

than 5%. The structure of the BMG samples before and after wear tests was characterized by using a Rigaku D/MAX-RB X-ray diffractometer (XRD) with a monochromatic $CuK\alpha$ radiation. After the wear tests, all the BMG sample surfaces were examined in a scanning electron microscope (SEM, FEI Helios Nanolab600i) or a 3-D laser scanning confocal microscope (LSCM, Phenom Pro X) in order to elucidate the wear mechanism of BMGs.

RESULTS AND DISCUSSION

Figure 1A shows the XRD pattern obtained from the as-cast Ti-based BMG sample. For the purpose of comparison, the XRD patterns of the Ti-based BMG samples after high-temperature wear tests at different temperatures and different loads are shown in **Figures 1B,C,D**. As can be seen, all XRD patterns of the studied BMG samples before and after high-temperature wear tests consist of only two broad diffraction maxima, without any sharp Bragg peaks corresponding to crystalline phase in the 2θ ranging $20 \sim 90$, typical of a glassy structure. This suggests that there is no wear-induced crystallization and the studied Ti-based BMG sample maintains its amorphous structure after high-temperature wear tests.

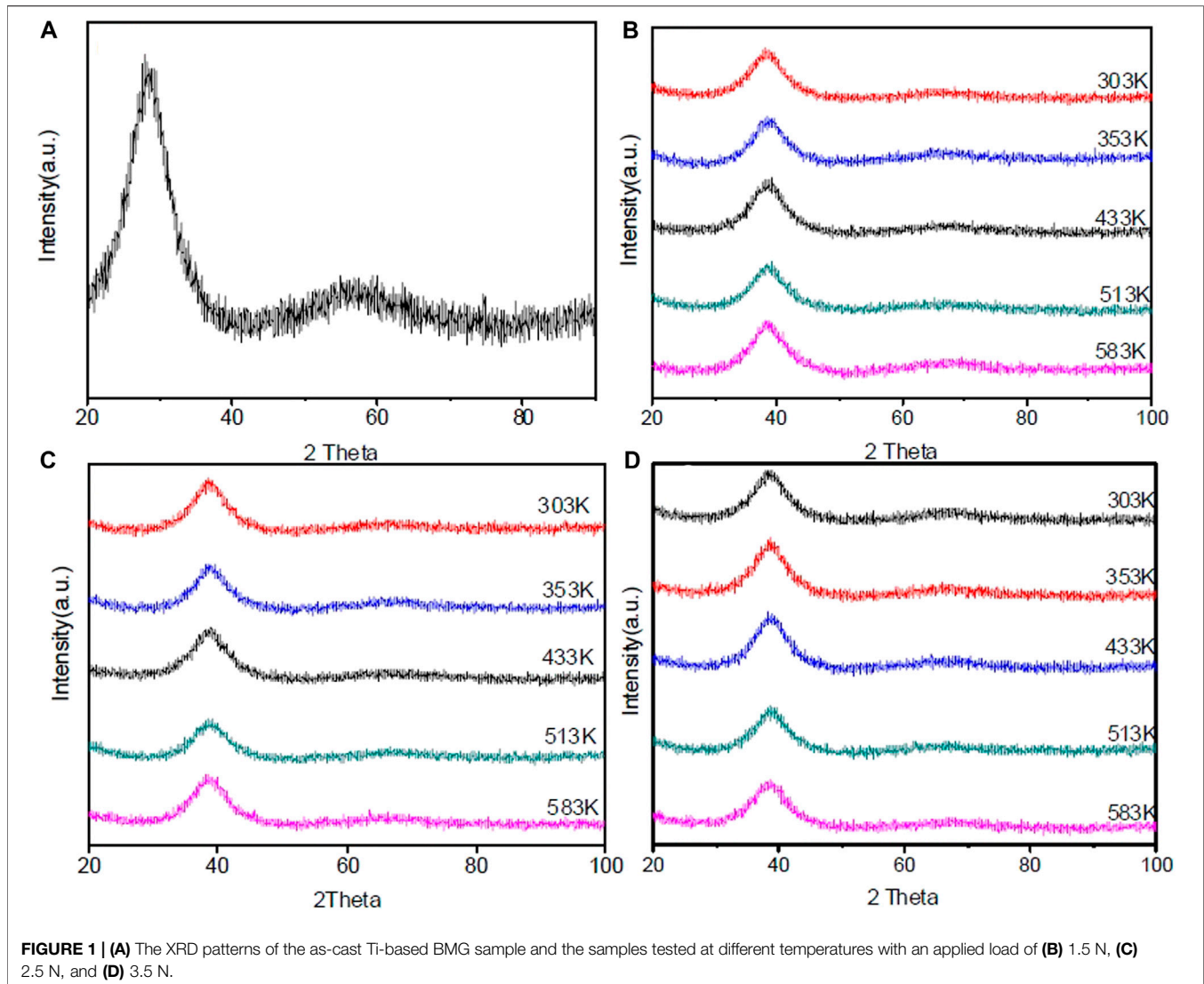
The COF is defined as the ratio of the force maintaining contact between a surface and an object to the frictional force resisting the motion of the object, and can be effectively used to evaluate the wear resistance of the testing materials (Zhong et al., 2015). **Figure 2** shows the COF of the studied Ti-based BMG as a function of the testing temperatures at an applied load of 1.5, 2.5, and 3.5 N. The COF value of the studied Ti-based BMG obtained at the steady state is 0.191, 0.232, 0.260, 0.282, and 0.332 for the testing temperature of 303, 353, 433, 513, and 583 K at an applied load of 1.5 N, respectively, as seen in **Figure 2A**. For the applied loads of 2.5 (**Figure 2B**) and 3.5 N (**Figure 2C**) the COF value shows a similar trend, that is, a higher testing temperature causes a higher COF value. It is generally accepted that a smaller COF value suggests a higher wear resistance because more energy is usually required to remove the same volume (Yang et al., 2008). Clearly, the wear rate of the studied Ti-based BMG alloy increased with increase in the testing temperature. Meanwhile, the COF was found to increase with the applied normal load, revealing that the wear rate gradually increases with increasing the applied normal load.

For the studied Ti-based BMG, its glass transition temperature and crystallization temperature are 603 and 654 K, respectively (Huang et al., 2010a). This means that the selected temperatures in this study are lower than the glass transition temperature, T_g . It is found that for the studied Ti-based BMG, when the testing temperature is lower than T_g , its strength, σ , follows the below relation (Huang et al., 2008):

$$\sigma/E = -0.0066T/T_g + 0.0206, \quad (1)$$

where E is Young's modulus and T is the testing temperature.

This means that a lower temperature yields a higher strength for the studied BMG. The relationship between wear resistance and the hardness value, H , can be described as follows:

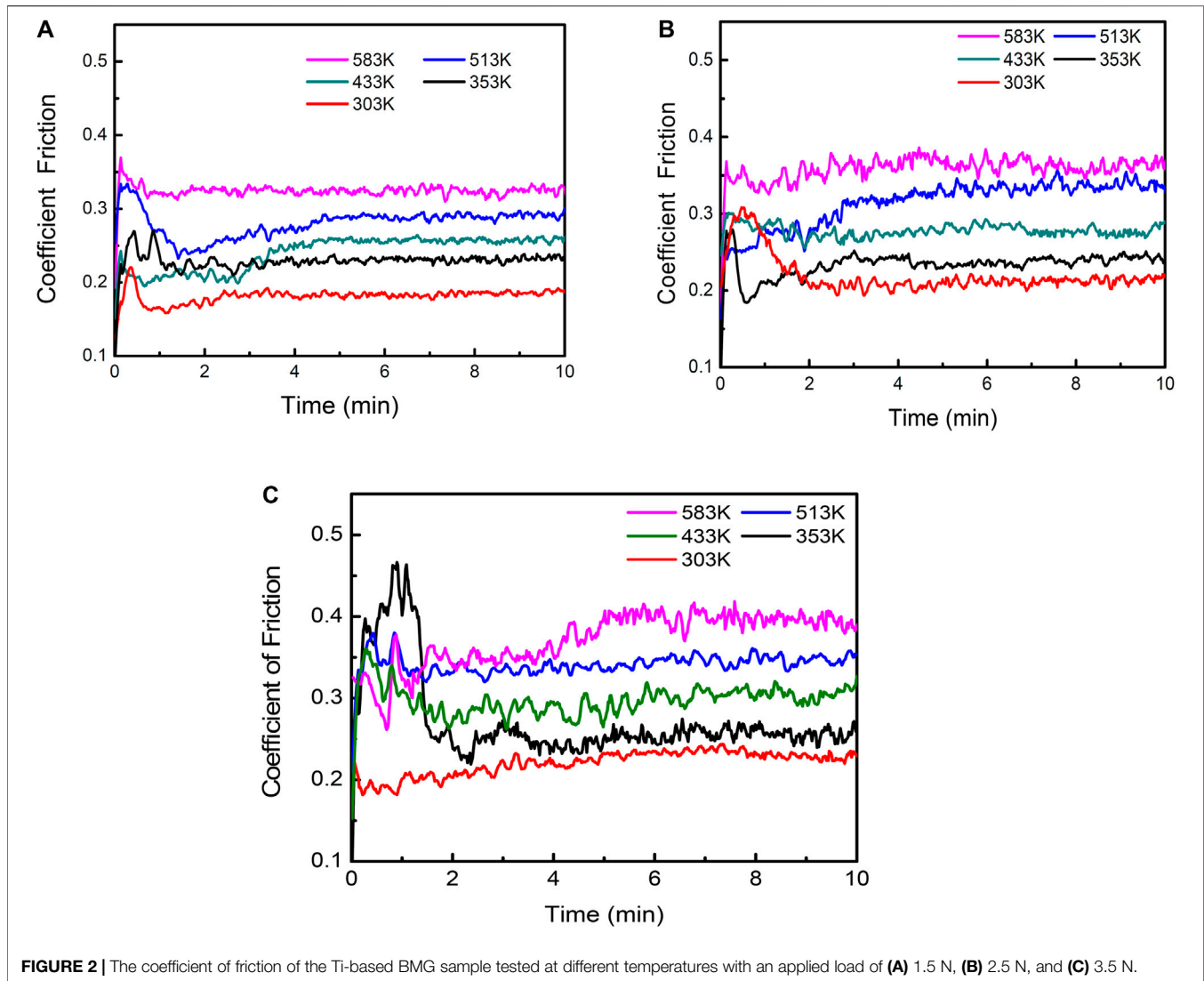


$$R_w = H/K, \quad (2)$$

where R_w is the wear resistance coefficient, in the unit of Pa, and K is a dimensionless constant. Following Tabor (Tabor, 1951), the hardness of a metallic glass is approximately proportional to its strength, with a ratio of ~ 3 (Yang et al., 2007). Accordingly, a higher temperature will result in lower strength and hardness, and thus a lower wear resistance, agreeing well with the results shown in **Figure 2**.

To gain further information regarding the wear mechanism of the studied Ti-based BMG at elevated temperatures, the worn sample surfaces after friction tests at different temperatures were examined by SEM. **Figure 3** shows the corresponding SEM images of the worn surfaces of the studied Ti-based BMG samples after 10 min contact sliding at different temperatures, with an applied load of 1.5 N. The surface of the Ti-based BMG sample after the wear tests at room temperature (303 K) consists of numerous plowed grooves parallel to the sliding direction, which is a typical morphology of a brittle

material induced by abrasive wear (see **Figure 3A**). Meanwhile, a large number of cotton-like wear debris appear on the worn surface, implying the occurrence of a great inhomogeneous shear deformation during wear tests. The worn surface of the sample tested at 353 K showed the similar feature consisting of a lot of grooves and cotton-like wear debris (see **Figure 3B**), but becomes a little smoother than that tested at 303 K. For the Ti-based BMG sample tested at 433 (**Figure 3C**), 513 (not shown here), and 583 K (**Figure 3D**), viscous flow appears on the worn surface instead of abrasive grooves, revealing that adhesion wear dominates the wear mechanism. Especially for 583 K, the worn surface of the studied Ti-based BMG sample consists of numerous extruded/ploughed fins. Another important phenomenon is that melting patterns can be found on all the worn sample surfaces after wear tests. The friction heat generated during the wear tests made the instant temperature between the Si_3N_4 ceramic balls and plates exceed the melting point of the studied Ti-based BMG alloy. Although to measure



in situ such instant temperature is a big challenge, some literatures have already stated that the rate of heat propagation is fast (Faupel et al., 2003). This could be the intrinsic reason why the melting phenomena on the worn sample surfaces were examined on the SEM images although no crystallization was indicated by the XRD patterns shown in **Figure 1**.

Figure 4A shows the typical 3-D LSCM images of the worn sample surfaces after wear tests at 303 K. The color evolution from blue to red indicates the profile evolution from low to high. To quantitatively study the deformation features after elevated temperature wear tests, the mean surface roughness (R_a) was measured to be 4.456, 4.423, 3.725, 3.276, and 2.749 μm for the sample tested at 303, 353, 433, 513, and 583 K, respectively, as plotted in **Figure 4B**, according to these LSCM images. It is evident that within the investigated temperature range, R_a decreases with increasing temperature. That means, the high temperature wear test causes a smoother sample surface.

The above observations on the surface morphology change suggest that the wear mode has undergone a transition from brittle to ductile as the testing temperature increases from 303 to 583 K. Testing temperature rise to a certain degree makes the studied Ti-based BMG more ductile and softer, and causes a lower surface roughness, as shown in **Figure 4B**.

SUMMARY

In summary, the wear tests of a Ti-based BMG at elevated temperatures were studied. The effect of the testing temperature and normal load on the wear behaviors was discussed. The studied Ti-based BMG retained its glassy structure after high-temperature wear. The wear rate increases with increasing the testing temperature and the applied normal load. The wear mechanism evolves from the abrasive to adhesive mode, and the sample surface becomes smoother as the testing temperature increases.

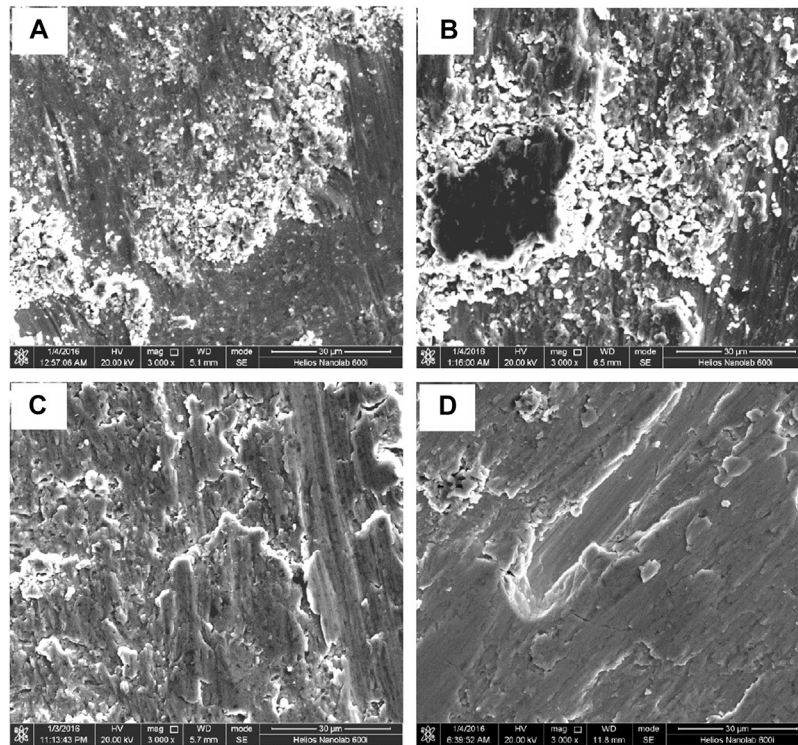


FIGURE 3 | The worn surface of the Ti-based BMG samples tested at (A) 303 K (B) 353 K, (C) 433 K, and (D) 583 K with an applied load of 1.5 N.

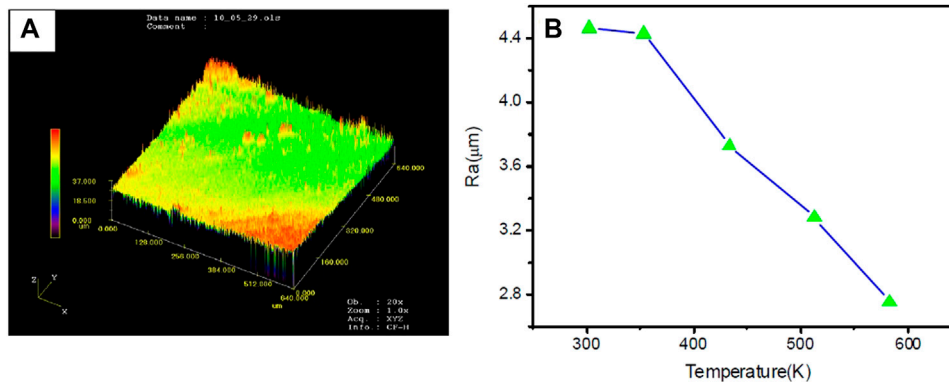


FIGURE 4 | (A) The typical LSCM image of the Ti-based BMG samples tested at 303 K and (B) the surface roughness of the samples as a function of the testing temperatures.

DATA AVAILABILITY STATEMENT

The original contributions presented in the study are included in the article/Supplementary Material; further inquiries can be directed to the corresponding author.

AUTHOR CONTRIBUTIONS

YH, FC, CH, and LW proposed the idea and wrote the manuscript; LW prepared the samples; FC and LW carried

out the experiments; YH, FC, CH, ZN, HF, LW, and JS revised and corrected the article; YH, FC, HC, and LW analyzed the data. All authors discussed the results and reviewed the manuscript.

FUNDING

This work was financially supported by the National Natural Science Foundation of China (NSFC) under Grant nos. 51871076, 51671070, 52071118, and 51827801.

REFERENCES

- Axinte, E. (2012). Metallic Glasses from “Alchemy” to Pure Science: Present and Future of Design, Processing and Applications of Glassy Metals. *Mater. Des.* 35, 518–556. doi:10.1016/j.matdes.2011.09.028
- Duan, H. T., Tu, J. S., Du, S. M., Kou, H. C., Li, Y., Wang, J. P., et al. (2011). Tribological Properties of Ti₄₀Zr₂₅Ni₈Cu₉Be₁₈ Bulk Metallic Glasses under Different Conditions. *Mater. Des.* 32, 4573–4579. doi:10.1016/j.matdes.2011.04.018
- Edwards, K. L., Axinte, E., and Tabacaru, L. L. (2013). A Critical Study of the Emergence of Glass and Glassy Metals as “green” Materials. *Mater. Des.* 50, 713–723. doi:10.1016/j.matdes.2013.03.070
- Faupel, F., Frank, W., Macht, M.-P., Mehrer, H., Naundorf, V., Rätzke, K., et al. (2003). Diffusion in Metallic Glasses and Supercooled Melts. *Rev. Mod. Phys.* 75, 237–280. doi:10.1103/RevModPhys.75.237
- Greer, A. L. (1995). Metallic Glasses. *Science* 267, 1947–1953. doi:10.1126/science.267.5206.1947
- Greer, A. L., Rutherford, K. L., and Hutchings, I. M. (2002). Wear Resistance of Amorphous Alloys and Related Materials. *Int. Mater. Rev.* 47, 87–112. doi:10.1179/095066001225001067
- Han, X., Ding, F., Qin, Y., Wu, D., Xing, H., Shi, Y., et al. (2018). Compositional Dependence of Crystallization Kinetics in Zr-Ni-Al Metallic Glasses. *Vacuum* 151, 30–38. doi:10.1016/j.vacuum.2018.02.001
- Hua, N., Huang, Y., Zheng, Z., Huang, Y., Su, M., Liao, Z., et al. (2017). Tribological and Corrosion Behaviors of Mg_{56.5}Cu₂₇Ag₅Dy_{11.5} Bulk Metallic Glass in NaCl Solution. *J. Non-Crystalline Sol.* 459, 36–44. doi:10.1016/j.jnoncrysol.2016.12.031
- Huang, D., Li, R., Huang, L., Ji, V., and Zhang, T. (2011). Fretting Wear Behavior of Bulk Amorphous Steel. *Intermetallics* 19, 1385–1389. doi:10.1016/j.intermet.2011.04.014
- Huang, Y., Chiu, Y. L., Shen, J., Sun, Y., and Chen, J. J. J. (2010). Mechanical Performance of Metallic Glasses during Nanoscratch Tests. *Intermetallics* 18, 1056–1061. doi:10.1016/j.intermet.2010.02.002
- Huang, Y., Fan, H., Wang, D., Sun, Y., Liu, F., Shen, J., et al. (2014). The Effect of Cooling Rate on the Wear Performance of a ZrCuAlAg Bulk Metallic Glass. *Mater. Des.* 58, 284–289. doi:10.1016/j.matdes.2014.01.067
- Huang, Y., Khong, J. C., Connolly, T., and Mi, J. (2014). The Onset of Plasticity of a Zr-Based Bulk Metallic Glass. *Int. J. Plasticity* 60, 87–100. doi:10.1016/j.ijplas.2014.05.003
- Huang, Y., Shen, J., Chen, J. J. J., and Sun, J. (2009). Critical Cooling Rate and Thermal Stability for a Ti-Zr-Ni-Cu-Be Metallic Glass. *J. Alloys Compounds* 477, 920–924. doi:10.1016/j.jallcom.2008.11.017
- Huang, Y., Shen, J., Sun, J., and Zhang, Z. (2008). Enhanced Strength and Plasticity of a Ti-Based Metallic Glass at Cryogenic Temperatures. *Mater. Sci. Eng. A* 498, 203–207. doi:10.1016/j.msea.2008.08.010
- Huang, Y., Shen, J., Sun, Y., Sun, J., and Chen, J. J. J. (2010). High Temperature Deformation Behaviors of Ti₄₀Zr₂₅Ni₃Cu₁₂Be₂₀ Bulk Metallic Glass. *J. Alloys Compounds* 504, S82–S85. doi:10.1016/j.jallcom.2010.02.163
- Hubek, R., Hilde, S., Davani, F. A., Golkia, M., Shrivastav, G. P., Divinski, S. V., et al. (2020). Shear Bands in Monolithic Metallic Glasses: Experiment, Theory, and Modeling. *Front. Mater.* 7, 144. doi:10.3389/fmats.2020.00144
- Ishida, M., Takeda, H., Nishiyama, N., Kita, K., Shimizu, Y., Saotome, Y., et al. (2007). Wear Resistivity of Super-precision Microgear Made of Ni-Based Metallic Glass. *Mater. Sci. Eng. A* 449–451, 149–154. doi:10.1016/j.msea.2006.02.300
- Khun, N. W., Yu, H., Chong, Z. Z., Tian, P., Tian, Y., Tor, S. B., et al. (2016). Mechanical and Tribological Properties of Zr-Based Bulk Metallic Glass for Sports Applications. *Mater. Des.* 92, 667–673. doi:10.1016/j.matdes.2015.12.050
- Li, J. B., Lin, H. C., Jang, J. S. C., Kuo, C. N., and Huang, J. C. (2013). Novel Open-Cell Bulk Metallic Glass Foams with Promising Characteristics. *Mater. Lett.* 105, 140–143. doi:10.1016/j.matlet.2013.04.071
- Li, M.-F., Liao, B., Wang, Y.-G., and Yang, L. (2019). Structural Mechanisms of the High Glass-Forming Ability in CuZrTiPd Metallic Glass. *J. Mater. Sci.* 54, 14209–14217. doi:10.1007/s10853-019-03890-1
- Liu, L., Song, H., Zhao, X.-J., Du, W., and Zhang, T. (2018). “Extended” Shear Bands in Interior of Pd-Based Bulk Metallic Glasses. *Rare Met.* 37, 54–58. doi:10.1007/s12598-015-0563-9
- Louzguine-Luzgin, D. V., Nguyen, H. K., Nakajima, K., Ketov, S. V., and Trifonov, A. S. (2016). A Study of the Nanoscale and Atomic-Scale Wear Resistance of Metallic Glasses. *Mater. Lett.* 185, 54–58. doi:10.1016/j.matlet.2016.08.035
- Louzguine-Luzgin, D. V., Zadorozhnyy, V. Y., Ketov, S. V., Wang, Z., Tsarkov, A. A., and Greer, A. L. (2017). On Room-Temperature Quasi-Elastic Mechanical Behaviour of Bulk Metallic Glasses. *Acta Materialia* 129, 343–351. doi:10.1016/j.actamat.2017.02.049
- Lu, Y., Huang, G., Wang, Y., Li, H., Qin, Z., and Lu, X. (2018). Crack-free Fe-Based Amorphous Coating Synthesized by Laser Cladding. *Mater. Lett.* 210, 46–50. doi:10.1016/j.matlet.2017.08.125
- Ma, M., Liu, R., Xiao, Y., Lou, D., Liu, L., Wang, Q., et al. (2004). Wear Resistance of Zr-Based Bulk Metallic Glass Applied in Bearing Rollers. *Mater. Sci. Eng. A* 386, 326–330. doi:10.1016/j.msea.2004.07.05410.1016/s0921-5093(04)00973-6
- Maddala, D. R., Mubarak, A., and Hebert, R. J. (2010). Sliding Wear Behavior of Cu₅₀Hf_{41.5}Al_{8.5} Bulk Metallic Glass. *Wear* 269, 572–580. doi:10.1016/j.wear.2010.06.004
- Matthews, D. T. A., Ocelik, V., and de Hosson, J. T. M. (2007). Tribological and Mechanical Properties of High Power Laser Surface-Treated Metallic Glasses. *Mater. Sci. Eng. A* 471, 155–164. doi:10.1016/j.msea.2007.02.119
- Prakash, B. (2005). Abrasive Wear Behaviour of Fe, Co and Ni Based Metallic Glasses. *Wear* 258, 217–224. doi:10.1016/j.wear.2004.09.010
- Rahaman, M. L., Zhang, L. C., and Ruan, H. H. (2014). Effects of Environmental Temperature and Sliding Speed on the Tribological Behaviour of a Ti-Based Metallic Glass. *Intermetallics* 52, 36–48. doi:10.1016/j.intermet.2014.03.011
- Rahaman, M. L., Zhang, L., Liu, M., and Liu, W. (2015). Surface Roughness Effect on the Friction and Wear of Bulk Metallic Glasses. *Wear* 332–333, 1231–1237. doi:10.1016/j.wear.2014.11.030
- Schuh, C., Hufnagel, T., and Ramamurty, U. (2007). Mechanical Behavior of Amorphous Alloys. *Acta Materialia* 55, 4067–4109. doi:10.1016/j.actamat.2007.01.052
- Shakur Shahabi, H., Scudino, S., Kaban, I., Stoica, M., Rütt, U., Kühn, U., et al. (2015). Structural Aspects of Elasto-Plastic Deformation of a Zr-Based Bulk Metallic Glass under Uniaxial Compression. *Acta Materialia* 95, 30–36. doi:10.1016/j.actamat.2015.05.011
- Sun, J. F., Huang, Y. J., Shen, J., Wang, G., and McCartney, D. G. (2006). Superplastic Formability of a Zr-Ti-Ni-Cu-Be Bulk Metallic Glass. *J. Alloys Compounds* 415, 198–203. doi:10.1016/j.jallcom.2005.08.018
- Tabor, D. (1951). *The Hardness of Metals*. London: Oxford University Press.
- Wang, G., Fan, H. B., Huang, Y. J., Shen, J., and Chen, Z. H. (2014). A New TiCuHfSi Bulk Metallic Glass with Potential for Biomedical Applications. *Mater. Des.* (1980–2015) 54, 251–255. doi:10.1016/j.matdes.2013.08.075
- Yang, F., Geng, K., Liaw, P., Fan, G., and Choo, H. (2007). Deformation in a Zr₅₇Ti₅Cu₂₀Ni₈Al₁₀ Bulk Metallic Glass during Nanoindentation. *Acta Materialia* 55, 321–327. doi:10.1016/j.actamat.2006.06.063
- Yang, J., Ma, J., Bi, Q., Liu, W., and Xue, Q. (2008). Tribological Properties of Fe₃Al Material under Water Environment. *Mater. Sci. Eng. A* 490, 90–94. doi:10.1016/j.msea.2008.01.024
- Yang, N., Yi, J., Yang, Y. H., Huang, B., Jia, Y. D., Kou, S. Z., et al. (2020). Temperature Effect on Fracture of a Zr-Based Bulk Metallic Glass. *Materials* 13, 2391. doi:10.3390/ma13102391
- Zhao, J., Gao, M., Ma, M., Cao, X., He, Y., Wang, W., et al. (2018). Influence of Annealing on the Tribological Properties of Zr-Based Bulk Metallic Glass. *J. Non-Crystalline Sol.* 481, 94–97. doi:10.1016/j.jnoncrysol.2017.10.033
- Zheng, W., Huang, Y. J., Wang, G. Y., Liaw, P. K., and Shen, J. (2011). Influence of Strain Rate on Compressive Deformation Behavior of a Zr-Cu-Ni-Al Bulk Metallic Glass at Room Temperature. *Metall. Mat. Trans. A* 42, 1491–1498. doi:10.1007/s11661-011-0632-0
- Zhong, H., Chen, J., Dai, L., Yue, Y., Zhang, Z., Zhang, X., et al. (2015). Tribological Behaviors of Zr-Based Bulk Metallic Glass versus Zr-Based Bulk Metallic Glass under Relative Heavy Loads. *Intermetallics* 65, 88–93. doi:10.1016/j.intermet.2015.06.002

Conflict of Interest: The authors declare that the research was conducted in the absence of any commercial or financial relationships that could be construed as a potential conflict of interest.

Copyright © 2021 Cao, Huang, He, Fan, Wei, Ning and Sun. This is an open-access article distributed under the terms of the Creative Commons Attribution License (CC BY). The use, distribution or reproduction in other forums is permitted, provided the original author(s) and the copyright owner(s) are credited and that the original publication in this journal is cited, in accordance with accepted academic practice. No use, distribution or reproduction is permitted which does not comply with these terms.